7. В.Д. Баскаков, О.В. Зарубина, К.А. Карнаухов, В.А. Тарасов. Математическое моделирование процесса соударения плоских струй идеальной жидкости Вестник Московского государственного технического университета им. Н.Э. Баумана. Серия: Естественные науки. 2016. № 2 (65). С. 79-90.
8. Н.А. Асмоловский, В.Д. Баскаков, В.А. Тарасов Численно-аналитическая оценка аэродинамических коэффициентов удлиненных тел сложной формы методом Ньютона. Вестник Московского государственного технического университета им. Н.Э. Баумана. Серия: Машиностроение. 2014. № 4. С. 109-122.

ANALYZING THE INFLUENCE OF THE THICKNESS VARIATION OF MENISCUS LINERS ON FORMING WRINKLES IN THE AFTERBODY OF EXTENDED EXPLOSIVELY FORMED PENETRATORS

M.A. Baburin[1], V. D. Baskakov[1], S.V. Yeliseev[2], O.V. Zarubina[1], K.A. Karnaukhov[1], V.A. Tarasov[1]

[1] BMSTU named after N.E. Bauman, Moscow, Russia
[2] NIMI named after V.V. Bahirev, Moscow, Russia

Explosively formed projectiles are widely used nowadays. The working principle of such charges is based on the collapse of the meniscus liner by detonation products, which results in the formation of an explosively formed penetrator (EFP) [1]. Hitting large objects from a big distance is better achieved by using more promising extended EFP-s ($l/d \geq 2$, where l – EFP length, d – EFP diameter); they can help penetrate the armor over caliber; such elements, however, are poorly regulated while in flight because of their length, technological inaccuracies and external factors. In order to improve aerodynamic and ballistic characteristics, various methods are applied, most of them are constructive and connected with creating a folded EFP afterbody by altering the body, liner, applying pillows, and multipoint initiation.

There is a whole range of papers dedicated to studying the formation of the folded afterbody of the extended EFP-s [2-5]. Thus, the main rules of forming a linear folded EFP afterbody by using multipoint initiation are described in the papers [2, 3]. Paper [4] shows that to form a folded EFP afterbody one can use meniscus liners which have wave-shaped meridian irregularities on the inner or the outer surfaces of the liner. Of much interest is the paper which shows the data on the the angular rotation velocity rate of the extended EFP-s with a diagonal folded stabilizing fin in the afterbody, which were formed by applying pillows between the HE of the charge and its liner [5]. The aim of this work is to establish the patterns of formation of the diagonal wrinkles in the EFP from the liners of variable thickness in circumferential direction and to assess the angular rotation velocity rate, as well as the aerodynamic characteristics of the EFP.

The patterns of formation of the EFP were established using 3D numerical modeling in the program complex LS-DYNA in Lagrangian coordinates. The key modeling feature was using a 4-nodular tetrahedron (ELFORM-13) as the type of the finite element, as well as using a special computational grid in order to suppress circuit perturbations in the EFP afterbody [6]. Initial and end conditions, material models, state equations were selected according to the recommendations from works [2-4, 7].

To study the wrinkle formation processes lab charges constructed by NIMI were used; they were 70 mm in diameter ($d_з = 70$ mm) with the initiation point on the axis and differed in their liner geometry. The bodies (density, $\rho = 7{,}81$ g/cm^3, Young's modulus of elasticity, $E = 210$ GPa, Poisson's ratio, $\mu = 0{,}3$, dynamic yield limit, $Y_T = 250$MPa) and liners ($\rho = 7{,}85$ g/cm^3, $Y_T = 650$ MPa, shear modulus, $G = 80$ GPa) were made of ductile steel; as the material for the HE, TG40 composition was chosen

($\rho = 1{,}67$ g/cm^3, detonation velocity, $D = 7750$ m/s, pressure in the Chapman-Jouguet point, $P = 29{,}5$ GPa).

Explosive formed projectile liner №1. Diameter, $d_0 = 64$ mm, radius of liner curvature, $R_0 = 55$ mm, thickness, $\delta = 2{,}45$ mm, deflection, $\Delta H = 11{,}5$ mm.

Explosive formed projectile liner №2. Diameter, $d_0 = 64$ mm, radius of liner curvature, $R_0 = 49{,}8$ mm, thickness, $\delta = 2{,}2$ mm, deflection, $\Delta H = 12{,}3$ mm.

Explosive formed projectile liner №3. Diameter, $d_0 = 64$ mm, radius of liner curvature, $R_0 = 47{,}8$ mm, thickness, $\delta = 2{,}2$ mm, deflection, $\Delta H = 10{,}1$ mm.

At the first stage of numerical calculations the circuit wrinkling process was suppressed by altering the structure of the computational grid [6]; comparing with the experimental data has confirmed the computational values of the geometric and kinematic parameters of the axisymmetric EFP made out of the explosively formed projectile №1.

At the second stage, comparing the computations with the experiments confirmed the formation of the linear folded stabilizing fin out of the peripheral part of the explosive formed projectile meniscus liner №2, created by decreases in thickness ratio $\overline{\Delta\delta} = 0{,}14$ ($\overline{\Delta\delta} = \Delta\delta/\delta$, where $\Delta\delta$ is the thickness of decreases or increases) in the form of 6 circular segments ($n = 6$) on the inner surface repeating in circumferential direction. The circular segments were 50 mm in radius, while the distance between the central points of the segments and the liner was 72 mm. The shape and dimensional specifications have satisfactorily coincided, while the difference between the initial velocities was 11% (fig. 1).

The results allow for the computations to be considered adequate and numerical modeling to be used for conducting a detailed analysis of the processes of forming linear and diagonal wrinkles.

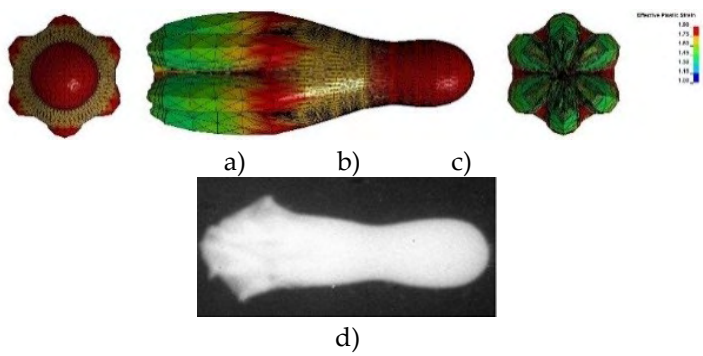

Figure 1. EFP-s created in numerical a) – c) and experimental d) ways at the moment of time $t = 149$ μs for the explosive formed projectile №2:
a) – front view; b) view from the cavity; c) view from the afterbody; d) roentgenography
The calculations are shown on the plastic strain rate field

Further research was conducted on the meniscus liners with non-symmetric and symmetric repeating contour in the shape of triangular areas in circumferential direction created on the inner or outer surface in the form of decreases and increases in thickness (fig. 2).

The results of numerical calculation have established that the EFP-s with a diagonal folded afterbody are formed out of the meniscus liners with a non-symmetric contour repeating in circumferential direction, while the EFP-s with a linear folded afterbody are formed out of the meniscus liners with a symmetric contour repeating in circumferential direction. It has been noted that a decrease in the size D_1 for the liners with areas of decreased thickness on the inner or outer surface leads to an increase in the plastic strain rate of the completed EFP in the forebody, while a decrease in the size D_2 for the liners with areas of increased thickness leads to a decrease in the plastic strain rate of the completed EFP in the forebody (fig. 3).

There has also been established a twisted rotation of the afterbody against the main body of the EFP, which may lead to the EFP's axial destruction (fig. 3). The results of the calculations have also shown that EFP-s with a folded afterbody tilted in different directions and varying in configuration are formed out of meniscus liners with areas of increased and decreased thickness (fig. 3 b, c).

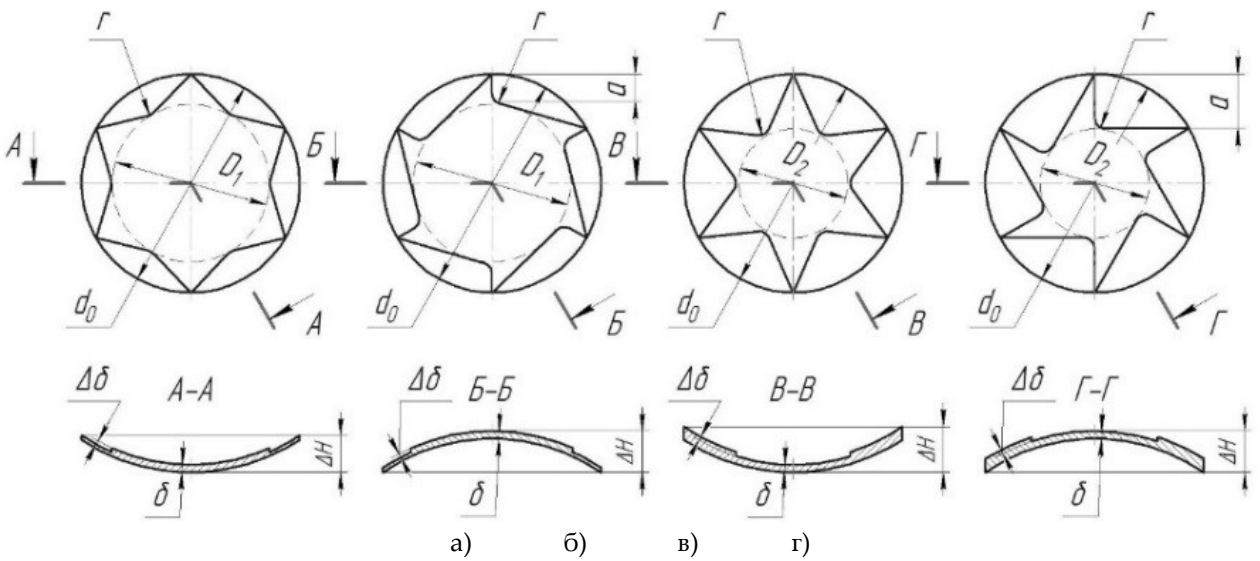

а) б) в) г)

Figure 2. Configurations of the liners of the explosively formed projectile №3 with diameter d_0:
a), b) – $a = d_0/8$, $D_1 = 3d_0/4$; c), d) – $a = d_0/4$, $D_2 = d_0/2$;
a) – a decrease in thickness on the inner surface; b) – a decrease in thickness on the outer surface; c) – an increase in thickness on the inner surface; d) an increase in thickness on the outer surface. r – edge radius

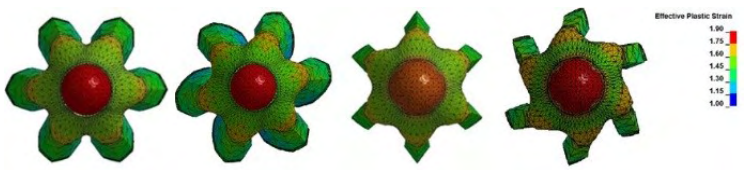

a) b) c) d)

Figure 3. Distribution of plastic strain on the configurations of the EFP of the explosively formed projectile №3 (front view) when changing thickness $\overline{\Delta\delta} = 0{,}05$ on the inner surface of the liner
$a = d_0/4$ and $D_2 = d_0/2$ at the moment of time $= 222\ \mu s$:
a), b) – decreases; c), d) – increases; a), c) symmetric contour; b), d) non-symmetric contour

There has been conducted a detailed analysis of the contour of ribs and cavities of the EFP wrinkles, formed out of liners with the areas of increased and decreased thickness at the periphery (fig. 3 b, d). Comparing the EFP-s has resulted in understanding that the tilt of a wrinkle may be characterized by two angles: angle α of the tilt about the axis of symmetry of the EFP and angle β of the tilt towards the body of the EFP (fig. 4).

In order to assess the influence of the protruding tilted afterbody on the rotation velocity a following approach has been proposed (fig. 4); it is based on the Newton's method and applicable in the conditions in question, $v(t) \geq 5M$, where M is the Mach number. The fin of a folded afterbody was, for the sake of simplicity, shown as a triangular shape. This approach has helped to calculate dependence of pressure on the surface on the angles α and β of flow interaction with the streamlined surface:

$$P_0(t) = n\rho_0 v^2(t) sin^2 \alpha cos^2 \beta, \quad (1)$$

where n – amount of wrinkles; ρ_0 – medium thickness; $v(t)$ – upcoming flow velocity.
Force moment affecting the diagonal folded afterbody was calculated as follows:

$$M_n(t) = n \int_{l_c}^{0} P_0(t) y_1(x_1) cos\alpha cos\beta \left(\frac{y_1(x_1)}{2} cos\beta + \frac{d_2}{2}\right) dx_1 \quad (2)$$

After plugging (1) into (2) and performing integration, the following expression was deduced for assessing the EFP's rotation velocity around the axis:

$$\omega(t) = \frac{M_n(t)}{J_0} t = n\rho_0 v^2(t) sin^2\alpha cos\alpha cos^3\beta \left(\frac{l_c h(\frac{h}{3}cos\beta + \frac{d_2}{2})}{2J_0} \right) t, \quad (3)$$

where J_0 – EFP's axial moment of inertia.

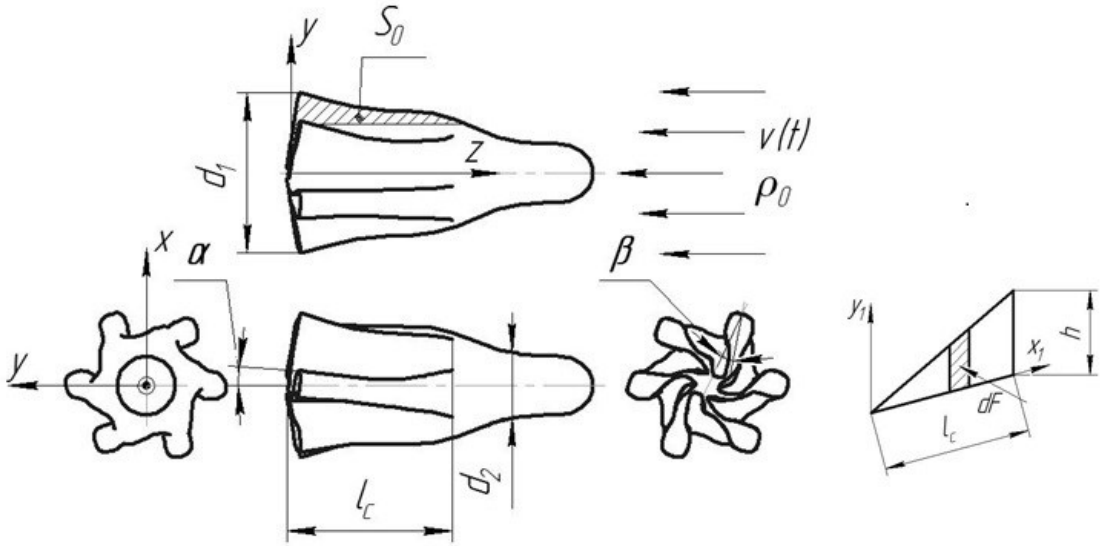

Figure 4. Computational scheme of the EFP
d_1 – diameter of the afterbody; d_2 – diameter of the forebody; l_c – length of the folded afterbody;
dF – elementary force affecting the wrinkle; S_0 –area affected by the upcoming flow;
h – height of the wrinkle

While analyzing (3) it should be noted that rotation rate ω is in direct dependence on the angle α (snap-back angle) and inverse dependence on the angle β (idle angle).

Approximate estimate of the EFP's rotation velocity was made according to the dependence (3); EFP-s were formed out of the liners with the areas of increased and decreased thickness (fig. 3 b, d). Resulting imputations of rotation velocity $\omega \approx 2300$ rad/s (fig. 3 b) and $\omega \approx 5300$rad/s (fig. 3 d) at the distance of 100 meters do not contradict the studies conducted before and gives the hope that rotation will be an additional factor in stabilizing EFP when flying towards the barrier [1].

Apart from estimating the EFP's rotation velocity, a calculation of the EFP's aerodynamic calculations is performed; the EFP in this case is formed out of the liners with decreases in thickness. The computations are made in a broad diapason of the attack angle α in the program complex SolidWorks Flow Simulation. This complex has gained a high reputation in evaluating aerodynamic characteristics of bodies for the velocity of the upcoming flow,$v(t) \geq 4$M, which is proven by the results of numerical calculations and experiments satisfactorily coinciding [8].

The result of the calculations shows aerodynamic characteristics of an axisymmetric EFP with a nominal conical skirt and an EFP with a linear and diagonal folded afterbody (fig. 3 a, b).

It has been established that the coefficient of the axial force c_x will be less for an EFP with a linear folded afterbody as compared with an EFP with a diagonal folded afterbody. The normal force coefficient c_y, the pitching moment coefficient m_z, center-of-pressure coordinate CP do not differ for both EFP types. It has also been stated that, for an EFP with a folded afterbody, the coefficient of the axial force c_x is 1,5…2 times less than for a nominal EFP with a developed conical afterbody, which has a positive result on the velocity of flying towards the object of destruction, although this element is less stable in flight excluding rotation (fig. 5).

Conclusions

1 EFP-s with a linear folded afterbody are formed out of meniscus liners, the peripheral part of which includes interlaced in circumferential direction areas of variable thickness in the form of symmetric segments. For the liners with areas of variable thickness on the periphery made in the form of non-symmetric segments, EFP-s with a folded diagonal afterbody are formed.

2 It is experimentally proven that a folded EFP afterbody is formed when using meniscus liners of variable thickness in circumferential direction.

3 Twisted rotation of the afterbody against the forebody of the EFP may lead to the EFP's axial destruction.

4 An algorithm of estimating the tilt angle of the EFP afterbody has been offered.

5 It has been established that when using the liners of variable thickness in circumferential direction the EFP rotation rate may reach the values of $\omega \approx 2300 \ldots 5300$ rad/s at the distance of 100 meters.

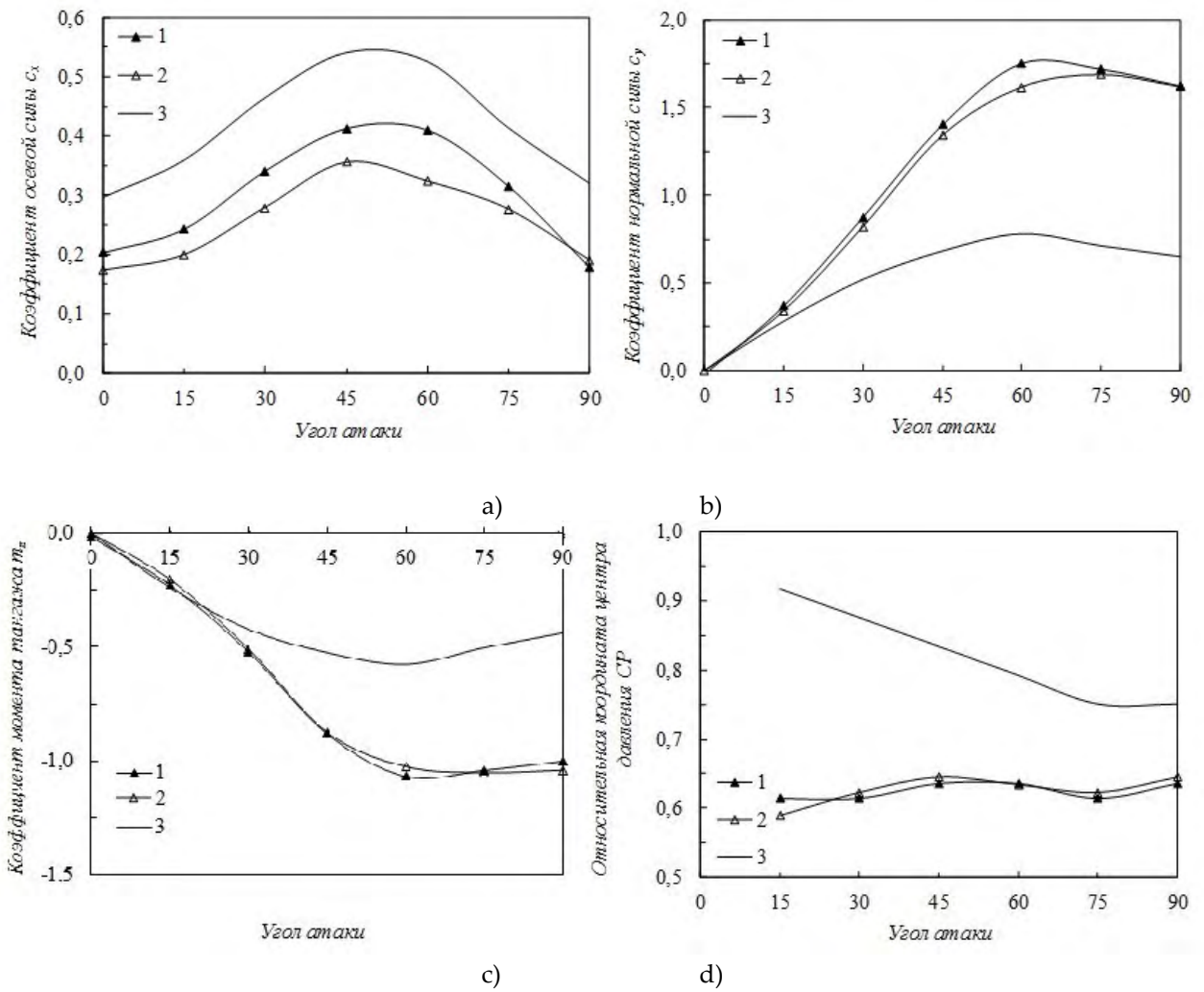

Figure 5. Graph of dependence of the aerodynamic characteristics on the EFP's angle of attack:
a) coefficient of the axial force c_x; b) normal force coefficient c_y;
c) pitching moment coefficient m_z;
d) center-of-pressure coordinate CP
1 – EFP with a diagonal folded afterbody (fig. 3 b); 2 – EFP with a linear folded afterbody (fig. 3 a);
3 – nominal axisymmetric EFP with a developed conical afterbody

References

1. Selivanov V.V. Munitions. In 2 t. Moscow, Publisher BMSTU, 2016, t. 1, 506 p.
2. Liu J., Gu W., Lu M., Xu H., Wu S. Formation of explosively formed penetrator with fins and its flight characteristics. Defense Technology, 2014, no. 10, pp. 119–123. DOI: 10.1016/j.dt.2014.05.00Mr.
3. Li R., Li W.B., Wang X.M., Li W.B. Effects of control parameters of three-point initiations on the formation of an explosively formed projectile with fins. Shock Waves, 2018, vol. 28, iss. 2, pp.191-204.
4. Asmolovsky N.A., Baskakov V.D., Tarasov V.A. The impact of periodic disturbances on the formation of high-speed rod elements // Proceedings of Higher Educational Institutions. Machine Buildings. 2013. № 8. pp. 8–14.
5. D. Bender, B. Chouk, R. Fong, W. Ng, B. Rice, E. Volkmann Explosively Formed Penetrators (EFP) with Canted Fins. 19th International Symposium on Ballistics (Interlaken, Swiitzerland, 7–11 May, 2001). Proceedings. In 3 volumes. 2001, vol. 2, pp. 755–762.
6. Johnson G.R., Stryk R.A. Some considerations for 3D EFP. Int. J. Impact Eng. 2006. Vol. 32, Iss.10, pp. 1621–1634.
7. Baskakov V.D., Zarubina O.V., Karnaukhov K.A., Tarasov V.A. Mathematical modeling of impact ideal liquid flat streams process // Bulletin BMSTU. Series: Natural sciences. 2016. № 2 (65). P. 79-90.
8 Asmolovsky N.A., Baskakov V.D., Tarasov V.A.Numerical and analytical extended bodies aerodynamics coefficients assessment of irregular shape by Newton's method. // Bulletin BMSTU. Series: Mechanical engineering. 2014. № 4. P. 109-122.

ВЛИЯНИЕ ВЫСОКОЭНЕРГЕТИЧЕСКОЙ ОБРАБОТКИ НА ВЗАИМОДЕЙСТВИЯ В СИСТЕМАХ SiC-Si_3N_4-C и Si_3N_4-C

С. В. Вихман[1], А.С. Козлов[1,2], П.В. Егорова[1],
А.А. Котомин [2], Г.В. Семашкин [2], С.А. Душенок [2]

[1]Санкт-Петербургский государственный технологический институт (технический университет), Санкт-Петербург, Россия
[2]Федеральное государственное унитарное предприятие «Специальное конструкторско-технологическое бюро «Технолог», Санкт-Петербург, Россия

Введение. В работе рассматривается возможность получения карбонитрида кремния на основе смесей SiC-Si_3N_4-C и Si_3N_4-C путем ударно-волновой активации.

Известно, что карбид и нитрид кремния имеют достаточно низкую (порядка 2 мол.% при T=1780°C) взаимную растворимость друг в друге. При этом, согласно данным термодинамического анализа [1], образование тройных соединений кремния в данной системе возможно, однако необходимо инициировать физико-химические взаимодействия компонентов [2]. Одним из перспективных методов механической активации является обработка порошков ударной волной. Данный метод заключается в накоплении структурных дефектов кристаллических решеток исходных веществ в результате высокоэнергетической активации.

Карбонитрид кремния является высокотемпературным материалом с рабочей температурой 1600°C. Благодаря своей высокой коррозионной стойкости, SiCN может использоваться в таких жестких термомеханических условиях, как двигатели ракет и самолетов. Карбонитрид кремния по своим характеристикам не уступает карбиду и нитриду кремния, которые на сегодняшний день являются основными в области ракето- и авиастроения (см. таблицу 1).

Также низкая плотность (ρ=2,3 г/см3) и высокая твердость (HV=20 ГПа) делает керамику SiCN перспективной в области бронематериалов.